Nonperturbative theory for the QED corrections to elastic electron-nucleus scattering

OPEN ACCESS
IOP Publishing
Journal of Physics G: Nuclear and Particle Physics
J. Phys. G: Nucl. Part. Phys. **51** (2024) 035105 (16pp)
https://doi.org/10.1088/1361-6471/ad1db3

Nonperturbative theory for the QED corrections to elastic electron-nucleus scattering

D H Jakubassa-Amundsen

Mathematics Institute, University of Munich, Theresienstrasse 39, D-80333 Munich, Germany

E-mail: dj@math.lmu.de

Received 18 August 2023, revised 28 November 2023
Accepted for publication 11 January 2024
Published 6 February 2024

Abstract

A potential for the vertex and self-energy correction is derived from the first-order Born theory. The inclusion of this potential in the Dirac equation, together with the Uehling potential for vacuum polarization, allows for a nonperturbative treatment of these quantum electrodynamical effects within the phase-shift analysis. Investigating the ^{12}C and ^{208}Pb targets, a considerable deviation of the respective cross section change from the Born results is found for the heavier target. It is shown that at low impact energies the dispersion effects play no role. Estimates for the correction to the beam-normal spin asymmetry and its accuracy at 5 MeV (for ^{208}Pb and ^{197}Au) are also provided.

Keywords: elastic electron scattering, QED corrections, spin asymmetry

1. Introduction

High-precision experiments with polarized electron beams [1–5] require a detailed knowledge of additional multiple photon processes which modify the Coulombic potential scattering cross section. In particular, for the planned parity-violation experiment at the new MESA accelerator, [6, 7] an accurate estimate of the degree of beam polarization, which will be measured with a Mott polarimeter after the pre-acceleration at 5 MeV, [8, 9] is necessary.

To the radiative corrections belong, besides dispersion and bremsstrahlung, the vacuum polarization and the vertex correction, renormalized by the self-energy and made infrared finite by the soft bremsstrahlung.

For vacuum polarization it is well-known that the addition of the Uehling potential to the Coulombic target field V_T, which arises from the nuclear charge distribution, provides a nonperturbative consideration of this quantum electrodynamical (QED) effect [10, 11]. It is the first nonvanishing term in the decomposition of the vacuum loop in powers of V_T [12]. Indeed, if the Uehling potential were treated to first order,[13] the respective transition amplitude would agree with Tsai's result [14, 15] from the first-order Born approximation.

The relation between the first-order Born amplitude and the underlying potential was recently applied in the context of the contribution to the beam-normal spin asymmetry, also known as Sherman function, [16] which results from dispersion. In their method, Koshchii *et al* [17] constructed an absorptive potential from the respective Born amplitude, to be included in the Dirac equation for the electronic scattering states, in order to provide a nonperturbative representation of the dispersive spin asymmetry.

In the present work this procedure is adopted for generating a potential $V_{\rm vs}$ for the vertex and self-energy (vs) correction from the respective first-order Born amplitude. Apart from the nonperturbative treatment of the cross section modifications induced by adding $V_{\rm vs}$ to V_T in the Dirac equation, this allows for a consistent estimate of the respective changes in the spin asymmetry. By considering a light (^{12}C) and a heavy (^{208}Pb) target nucleus and electrons with energies between 2 and 56 MeV, the QED corrections and their dependence on the employed model are investigated in a large region of momentum transfers.

The paper is organized as follows. In section 2 the vs potential is derived. Results for the QED modifications of the differential cross section and the spin asymmetry are given in section 3 for the two target nuclei. Dispersion corrections within the second-order Born approximation and accuracy estimates are also provided. Concluding remarks follow (section 4). Atomic units ($\hbar = m = e = 1$) are used unless indicated otherwise.

2. Theory

In the Born approximation, the differential cross section for the elastic scattering of a spin-polarized electron into the solid angle $\mathrm{d}\Omega_f$, which includes the QED corrections to lowest order,[18] is given by

$$\frac{\mathrm{d}\sigma^{B1}}{\mathrm{d}\Omega_f} = \frac{k_f}{k_i}\frac{1}{f_{\rm rec}}\sum_{\sigma_f}\left[\,|A_{fi}^{B1}|^2 + 2\,\mathrm{Re}\,\{A_{fi}^{*B1}(A_{fi}^{\rm vac} + A_{fi}^{\rm vs})\} + \frac{\mathrm{d}\sigma^{\rm soft}}{\mathrm{d}\Omega_f}\right], \qquad (2.1)$$

where it is summed over the final spin polarization σ_f of the electron. A_{fi}^{B1} is the first-order Born amplitude for potential scattering in the Coulombic target field V_T, which can be represented in terms of the nuclear charge form factor $F_L(|\boldsymbol{q}|)$,[19]

$$A_{fi}^{B1}(\boldsymbol{q}) = -\frac{2\sqrt{E_i E_f}}{c^2}\frac{Z}{\boldsymbol{q}^2}\,(u_{k_f}^{+(\sigma_f)}\,u_{k_i}^{(\sigma_i)})F_L(|\boldsymbol{q}|), \qquad (2.2)$$

where Z is the nuclear charge number and $u_{k_i}^{(\sigma_i)}$, $u_{k_f}^{(\sigma_f)}$ are, respectively, the free 4-spinors of the initial and final electronic states to the spin polarization σ_i, σ_f. Here and in the following k_i and k_f denote the moduli of the initial and final electron momenta $\boldsymbol{k}_i$ and $\boldsymbol{k}_f$, respectively. In (2.1), $A_{fi}^{\rm vac}$ and $A_{fi}^{\rm vs}$ are the lowest-order amplitudes for vacuum polarization and the vertex and self-energy correction, respectively. Recoil effects are considered by the prefactor $f_{\rm rec}^{-1}$ [13].

In lowest-order Born approximation, the vacuum polarization amplitude reads [15]

$$A_{fi}^{\rm vac} \;=\; \frac{1}{3\pi c}\left[\frac{3-v^2}{2}\,v\,\ln\frac{v+1}{v-1} \;+\; v^2 \;-\; \frac{8}{3}\right] A_{fi}^{B1}, \tag{2.3}$$

where $v=\sqrt{1-4c^2/q^2}$, and $q^2=(E_i-E_f)^2/c^2-\boldsymbol{q}^2$, with $\boldsymbol{q}=\boldsymbol{k}_i-\boldsymbol{k}_f$, is the squared 4-momentum transfer to the nucleus. E_i and E_f are the initial, respectively final, total energies of the scattering electron.

The lowest-order Born amplitude for the vertex correction, after eliminating the UV divergence by renormalizing with the help of the self energy, is given in terms of two parts, $A_{fi}^{\rm vs(1)}+A_{fi}^{\rm vs(2)}$, by [20, 21]

$$A_{fi}^{\rm vs} \;=\; \left[F_1^{\rm vs}(-q^2) \;+\; \frac{1}{2c}\,F_2^{\rm vs}(-q^2)R_{fi}\right] A_{fi}^{B1}. \tag{2.4}$$

The first part, $A_{fi}^{\rm vs(1)}$, is governed by the electric form factor,

$$\begin{aligned} F_1^{\rm vs}(-q^2) \;=\; \frac{1}{2\pi c}\Bigg[&\frac{v^2+1}{4v}\left(\ln\frac{v+1}{v-1}\right)\left(\ln\frac{v^2-1}{4v^2}\right)\\ &+\frac{2v^2+1}{2v}\ln\frac{v+1}{v-1}-2+\frac{v^2+1}{2v}\left\{\mathrm{Li}\left(\frac{v+1}{2v}\right)-\mathrm{Li}\left(\frac{v-1}{2v}\right)\right\}\Bigg] \;+\; \mathrm{IR}, \end{aligned} \tag{2.5}$$

where $\mathrm{Li}\,(x)=-\int_0^x \mathrm{d}t\frac{\ln|1-t|}{t}$ is the Spence function [21, 22]. IR denotes the infrared divergent term.

The second part of the vertex correction, $A_{fi}^{\rm vs(2)}$, is of magnetic origin and hence reduced by a factor $1/c$ (the fine-structure constant in atomic units). The magnetic form factor is given by[20]

$$F_2^{\rm vs}(-q^2) \;=\; \frac{1}{4\pi c}\,\frac{v^2-1}{v}\,\ln\frac{v+1}{v-1}, \tag{2.6}$$

and R_{fi} is defined by

$$(u_{k_f}^{+(\sigma_f)}\,u_{k_i}^{(\sigma_i)})\,R_{fi} \;=\; (u_{k_f}^{+(\sigma_f)}\,\gamma_0(\boldsymbol{\alpha}\cdot\boldsymbol{q})\,u_{k_i}^{(\sigma_i)}), \tag{2.7}$$

where $\boldsymbol{\alpha}$ and γ_0 refer to Dirac matrices.

The differential cross section for the soft bremsstrahlung reads in Born approximation

$$\frac{\mathrm{d}\sigma^{\rm soft}}{\mathrm{d}\Omega_f} \;=\; W_{fi}^{\rm soft}\,|A_{fi}^{B1}|^2 \tag{2.8}$$

with (correcting printing errors in [15] and [20])

$$\begin{aligned} W_{fi}^{\rm soft} = -\frac{1}{\pi c}\Bigg\{&2\ln\frac{2\omega_0}{c^2} \;+\; \frac{E_i}{k_i c}\ln\frac{c^2}{E_i+k_i c} \;+\; \frac{E_f}{k_f c}\ln\frac{c^2}{E_f+k_f c}\\ &-\Bigg[2\left(\ln\frac{2\omega_0}{c^2}\right)\frac{v^2+1}{2v}\ln\frac{v+1}{v-1}\\ &+c^4\beta\,\frac{1-q^2/(2c^2)}{\zeta(\beta E_i-E_f)}\Bigg(\frac{1}{4}\left(\ln\frac{E_i-k_i c}{E_i+k_i c}\right)^2-\frac{1}{4}\left(\ln\frac{E_f-k_f c}{E_f+k_f c}\right)^2\\ &+\mathrm{Li}\left(1-\beta\,\frac{E_i-k_i c}{\zeta}\right)-\mathrm{Li}\left(1-\frac{E_f-k_f c}{\zeta}\right)\\ &+\mathrm{Li}\left(1-\beta\,\frac{E_i+k_i c}{\zeta}\right)-\mathrm{Li}\left(1-\frac{E_f+k_f c}{\zeta}\right)\Bigg)\Bigg]\Bigg\} \;-\; 2\mathrm{IR}, \end{aligned} \tag{2.9}$$

where the cutoff frequency ω_0 of the soft photons and the following abbreviations are introduced,

$$\beta = 1 - \frac{q^2}{2c^2} + \sqrt{-\frac{q^2}{c^2}\left(1 - \frac{q^2}{4c^2}\right)}$$
$$\zeta = c^4\left[\beta\left(1 - \frac{q^2}{2c^2}\right) - 1\right]\frac{1}{\beta E_i - E_f}. \tag{2.10}$$

The validity of (2.9) for $W_{fi}^{\rm soft}$ is subject to the requirement that ω_0 is not too small ($\frac{1}{\pi c}|\ln\frac{\omega_0}{c^2}| \ll 1$ [12]). Due to mutual cancellations in (2.9), a very large integration step number for the Spence functions is necessary. For $-q^2/c^2 \gtrsim 100$, the much simpler asymptotic formula for $W_{fi}^{\rm soft}$ can be used, as e.g. given in [15] or [13]. Hard bremsstrahlung is disregarded in (2.1), since it is assumed that the resolution ΔE of the electron detector (which defines the upper limit of the photon frequency by $\omega_0 = \Delta E$) is below 1 MeV.

For the construction of a nonperturbative theory, the IR contributions in (2.5) and (2.9) are omitted because it is known that they cancel to all orders [22, 23]. In order to derive the potential $V_{\rm vs}$ for the vertex and self-energy process we note that there is a simple connection between the first-order Born amplitude and the potential by which it is generated. This is exemplified for the scattering amplitude A_{fi}^{B1} in (2.2) by relating the form factor to the Fourier transform of the target potential V_T,

$$F_L(|\boldsymbol{q}|) = -\frac{\boldsymbol{q}^2}{4\pi Z}\int \mathrm{d}\boldsymbol{r}\ \mathrm{e}^{\mathrm{i}\boldsymbol{q}\cdot\boldsymbol{r}}\, V_T(r). \tag{2.11}$$

Upon employing the inverse Fourier transform, this provides us with the basic relation between the first-order Born amplitude and the underlying potential,

$$V_T(r) = \frac{1}{(2\pi)^3}\int \mathrm{d}\boldsymbol{q}\ \mathrm{e}^{-\mathrm{i}\boldsymbol{q}\cdot\boldsymbol{r}}\, A_{fi}^{B1}(\boldsymbol{q})\Big/A_0,$$
$$A_0 = \frac{\sqrt{E_iE_f}}{2\pi c^2}\,(u_{k_f}^{+(\sigma_f)}\, u_{k_i}^{(\sigma_i)}). \tag{2.12}$$

For the determination of the desired potential $V_{\rm vs}$ only the first term, $A_{fi}^{{\rm vs}(1)}$, of $A_{fi}^{\rm vs}$ is considered, which usually is dominating by several orders of magnitude. Due to the proportionality of $A_{fi}^{{\rm vs}(1)}$ to the scattering amplitude A_{fi}^{B1}, formula (2.12) can be applied, defining $V_{\rm vs}$ by means of

$$V_{\rm vs}(r) = \frac{1}{(2\pi)^3}\int \mathrm{d}\boldsymbol{q}\ \mathrm{e}^{-\mathrm{i}\boldsymbol{q}\cdot\boldsymbol{r}}\, A_{fi}^{{\rm vs}(1)}\Big/A_0$$
$$\approx -\frac{2Z}{\pi}\int_0^\infty \mathrm{d}|\boldsymbol{q}|\ \frac{\sin(|\,\boldsymbol{q}\,|\,r)}{|\,\boldsymbol{q}\,|\,r}\, F_L(|\boldsymbol{q}|)\, F_1^{\rm vs}(-q^2). \tag{2.13}$$

When performing the angular integration, the weak dependence of $F_1^{\rm vs}$ on $E_i - E_f$ (and hence on the scattering angle ϑ_f) by means of recoil has been disregarded.

For the nonperturbative consideration of vacuum polarization and the main part of the vs correction, the Dirac equation with the additional potentials is solved,

$$[-\mathrm{i}c\boldsymbol{\alpha}\cdot\boldsymbol{\nabla} + \gamma_0 c^2 + V_T(r) + U_e(r) + V_{\rm vs}(r)]\psi(\boldsymbol{r}) = E\ \psi(\boldsymbol{r}), \tag{2.14}$$

where U_e is the Uehling potential [24].

3. Results

The Coulombic target potentials of ^{12}C and ^{208}Pb are generated from the Fourier-Bessel representation of the respective ground-state charge densities [25]. The electronic scattering state ψ is expanded in terms of partial waves which, together with their phase shifts, are determined with the help of the Fortran code RADIAL of Salvat *et al* [26]. Since the two additional potentials U_e and $V_{\rm vs}$ are of long range (as compared to the nuclear radius), they require matching points between the inner and outer radial solutions of the Dirac equation of the order of 2000 fm. The determination of the scattering amplitude involves weighted summations of the phase shifts,[18] which are performed with the help of a threefold convergence acceleration [27]. Hence it is sufficient to take up to 25 000 partial waves into account. Recoil is included in the phase-shift analysis in terms of a reduced collision energy $\sqrt{(E_i - c^2)(E_f - c^2)}$, in a similar way as done for excitation [28].

3.1. Differential cross sections

The Born QED results, based on (2.1), do not account for the Coulomb distortion in the amplitude A_{fi}^{B1}. This deficiency, crucial for the heavier nuclei, can easily be remedied by replacing A_{fi}^{B1} with the phase-shift result $f_{\rm coul}$ for potential scattering in the Coulomb field, but nevertheless retaining the first-order treatment of the QED effects. Following the suggestion of Maximon,[29] this is achieved by profiting from the explicit dependence of $A_{fi}^{\rm vac}$, $A_{fi}^{\rm vs} = A_{fi}^{vs(1)} + A_{fi}^{vs(2)}$ and $\mathrm{d}\sigma^{\rm soft}/\mathrm{d}\Omega_f$ on A_{fi}^{B1} and therefore making this replacement not only in the leading term of (2.1) but also in these QED contributions. Their respective change is denoted by a tilde, so that one is now dealing with $\tilde{A}_{fi}^{\rm vac}$, $\tilde{A}_{fi}^{\rm vs}$ and $\mathrm{d}\tilde{\sigma}^{\rm soft}/\mathrm{d}\Omega_f$, replacing $A_{fi}^{\rm vac}$, A_{fi}^{vs} and $\mathrm{d}\sigma^{\rm soft}/\mathrm{d}\Omega_f$ in (2.1). This leads to the distortion-modified Born cross section,

$$\frac{\mathrm{d}\sigma^{B1-C}}{\mathrm{d}\Omega_f} = \frac{k_f}{k_i}\frac{1}{f_{\rm rec}}\sum_{\sigma_f}\left[\,|f_{\rm coul}|^2 \;+ 2\,\mathrm{Re}\,\{f_{\rm coul}^*(\tilde{A}_{fi}^{\rm vac} + \tilde{A}_{fi}^{\rm vs})\} + \frac{\mathrm{d}\tilde{\sigma}^{\rm soft}}{\mathrm{d}\Omega_f}\right]. \tag{3.1}$$

By using (3.1) in the actual calculations, Coulomb distortion effects are reduced in the comparison with the nonperturbative QED results. Noting that $\tilde{A}_{fi}^{\rm vac}$ is, like $\tilde{A}_{fi}^{\rm vs}$, proportional to $f_{\rm coul}$, the expression on the rhs of (3.1) is proportional to the Coulombic cross section,

$$\frac{\mathrm{d}\sigma_{\rm coul}}{\mathrm{d}\Omega_f} = \frac{k_f}{k_i}\frac{1}{f_{\rm rec}}\sum_{\sigma_f}|f_{\rm coul}|^2. \tag{3.2}$$

This cross section is shown in figure 1 at 5 MeV and 40 MeV collision energy for both targets. For the extended ^{208}Pb nucleus the angular distribution at 40 MeV differs in shape from the one at 5 MeV (in contrast to the behaviour of ^{12}C) due to the onset of the diffraction structures.

On the other hand, the nonperturbative treatment of vacuum polarization and the main part of the vs process (leading to the scattering amplitude $f_{\rm vac+vs}$) results in the following expression for the differential cross section,

$$\frac{\mathrm{d}\sigma^{C}}{\mathrm{d}\Omega_f} = \frac{k_f}{k_i}\frac{1}{f_{\rm rec}}\sum_{\sigma_f}[\,|f_{\rm vac+vs}|^2 \;+\; W_{fi}^{\rm soft}\,|f_{\rm vac+vs}|^2 \;+\; 2\,\mathrm{Re}\{f_{\rm coul}^*\tilde{A}_{fi}^{\rm vs(2)}\}]. \tag{3.3}$$

The second term of $A_{fi}^{\rm vs}$ has been included within the Born approximation as given in (2.4), since it cannot be turned into a potential because R_{fi} depends explicitly on the initial and final electronic states. Its perturbative consideration is justified by its insignificance except at very low impact energies.

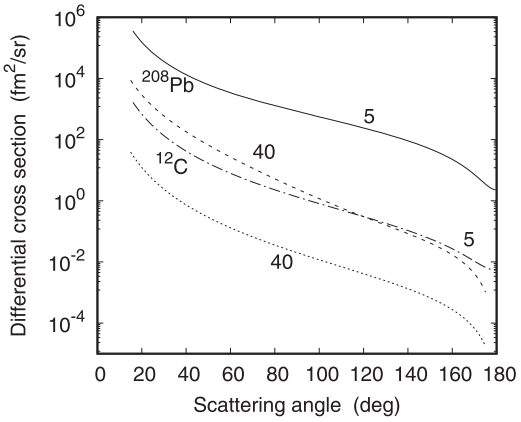

Figure 1. Differential cross section $\frac{\mathrm{d}\sigma_{\mathrm{coul}}}{\mathrm{d}\Omega_f}$ as a function of scattering angle ϑ_f for electrons of 5 MeV (———) and 40 MeV (– – – – –) colliding with ^{208}Pb. Included are results for electrons colliding with ^{12}C at 5 MeV (– · – · –) and 40 MeV (⋯ ⋯).

In the prescription (3.3) of the soft-bremsstrahlung cross section the fact has been accounted for that the cross section for emitting an additional soft photon during a certain scattering process is given by the cross section for this scattering process times a factor which describes the attachment of one soft-photon line to the respective diagram [30]. This factorization holds as long as the scattering process is undisturbed by this photon emission. In particular, the photon energy has to be sufficiently low ($\omega_0 \ll E_i - c^2$) and the change $\delta|\boldsymbol{q}|/|\boldsymbol{q}|$ of momentum transfer sufficiently small. This restricts the scattering angle by means of [18, 31]

$$\sin\frac{\vartheta_f}{2} \gg \frac{\omega_0 c^4}{4\,E_i^3}. \tag{3.4}$$

For the present cases of interest, both conditions are well satisfied. In particular, one has for $E_i - c^2 \gtrsim 1$ MeV and an energy resolution of at most 1% the requirement of $\vartheta_f \gtrsim 3°$. By using the Born factor W_{fi}^{soft} in (3.3) the approximation is made that this soft-photon line corresponds to a free electron, in the same spirit as the free-electron representation is used in the second-order Born theory of dispersion.

The effect of the QED processes is illustrated by considering the cross section change, defined with respect to the Coulombic cross section,

$$\Delta\sigma = \frac{\mathrm{d}\sigma/\mathrm{d}\Omega_f}{\mathrm{d}\sigma_{\mathrm{coul}}/\mathrm{d}\Omega_f} - 1, \tag{3.5}$$

where in the two cross sections occurring in (3.5) an additional averaging over the initial spin polarizaton σ_i is implemented. The relative cross section changes from the individual QED processes are additive, such that

$$\Delta\sigma^{B1-C} = \Delta\tilde{\sigma}^{\mathrm{vac}} + \Delta\tilde{\sigma}^{\mathrm{vs}} + \Delta\tilde{\sigma}^{\mathrm{soft}}, \tag{3.6}$$

and

$$\Delta\sigma^{C} = \Delta\sigma^{\mathrm{vac+vs}} + \Delta\sigma^{\mathrm{soft}}, \tag{3.7}$$

where the summands in (3.6) and (3.7) correspond to the contributions to $\Delta\sigma$ from the individual terms in (3.1) and (3.3), respectively. It should be noted that $\Delta\sigma^{B1-C}$ is

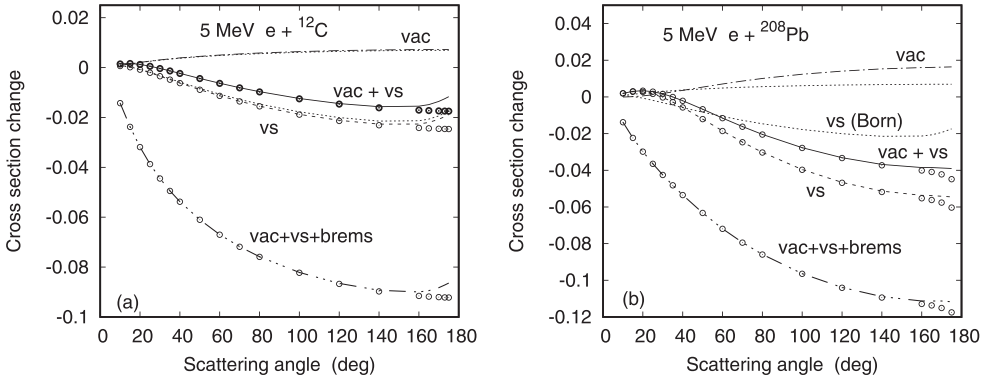

Figure 2. Relative cross section change $\Delta\sigma^C$ in 5 MeV (a) $e+^{12}$C and (b) $e+^{208}$Pb collisions as a function of scattering angle ϑ_f. Shown are the results for vacuum polarization ($-\cdot-\cdot-$), vertex and self-energy correction ($- - - -$) and the consideration of both (————-), as well as the additional inclusion of the soft-bremsstrahlung contribution for $\omega_0 = 0.05$ MeV ($- \cdots - \cdots -$). The respective results if $A_{fi}^{\mathrm{vs}(2)}$ is omitted are indicated by ($\circ$). Included are the Born results $\Delta\tilde{\sigma}^{\mathrm{vac}}$ for vacuum polarization ($\cdots\ \cdots$, upper line) and $\Delta\tilde{\sigma}^{\mathrm{vs}}$ for the vs correction ($\cdots\ \cdots$, lower line).

approximately target-independent, since the Coulombic cross section drops out and recoil effects in vacuum polarization, in F_1^{vs}, F_2^{vs} and in W_{fi}^{soft} are small.

The angular variation of the cross section change for 5 MeV electrons is displayed in figure 2. Apart from showing the combined influence of vacuum polarization and the vs effect, they are provided separately. This is done by retaining only their respective potential in (2.14) besides V_T. Bremsstrahlung is included by setting the detector resolution to 1% of the collision energy ($\omega_0 = 0.05$ MeV). For both targets it is seen that the effect of vacuum polarization is positive and very small, while the vertex and self-energy correction is basically negative and considerably larger at the backward angles. This confirms the earlier result of a partial cancellation of these two QED effects, obtained from exact bound-state calculations [12, 32]. However, the ratio of the absolute values of the vs and the vacuum-polarization correction is often beyond the factor of 2.5 predicted by these investigations. The inclusion of bremsstrahlung increases $|\Delta\sigma^C|$ considerably, the more so, the smaller ω_0 (caused by the logarithmic dependence on ω_0 in (2.9)). The inclusion of the magnetic vs contribution is unnecessary even for an energy as low as 5 MeV, except at $\vartheta_f \gtrsim 150°$ where it leads to a modification by up to 10% for ^{208}Pb and 30% for ^{12}C. When comparison is made with the Born results for the modifications by vacuum polarization and vs correction, there are large deviations from the nonperturbative results for the lead target, particularly in the backward hemisphere. For ^{12}C, the differences are much less perceptible, due to the smaller nuclear charge.

Figure 3 shows the energy dependence of the cross section change at a backward angle. Since the Coulombic cross section and hence its modifications are basically dependent on the momentum transfer (see, e.g. (2.2)), the angular and energy distributions of $\Delta\sigma^C$ are much alike. This is based on the fact that $|\boldsymbol{q}| \approx 2(E_i/c)\sin(\vartheta_f/2)$, such that increasing either E_i or ϑ_f result both in an increase of $|\boldsymbol{q}|$. The magnetic vs contribution is well below 0.5% for all energies $\gtrsim$20 MeV even at this large scattering angle.

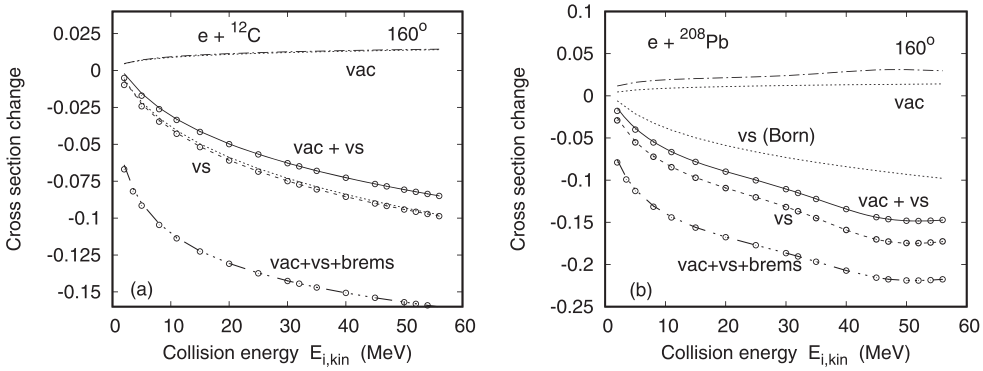

Figure 3. Relative cross section change $\Delta\sigma^C$ in (a) e+^{12}C and (b) e+^{208}Pb collisions at 160° as a function of collision energy $E_{\rm i,kin} = E_i - c^2$. The same line shapes are used as in figure 2. For the bremsstrahlung results, a detector resolution of 1% is used (i.e. $\omega_0 = 0.01\, E_{\rm i,kin}$).

3.2. Spin asymmetry

For incident electrons polarized perpendicular to $\boldsymbol{k}_i \times \boldsymbol{k}_f$, the Sherman function S is defined as the relative cross section difference when the initial spin is flipped from up ($\uparrow$) to down ($\downarrow$),

$$S = \frac{{\rm d}\sigma/d\Omega_f(\uparrow) - {\rm d}\sigma/d\Omega_f(\downarrow)}{{\rm d}\sigma/d\Omega_f(\uparrow) + {\rm d}\sigma/d\Omega_f(\downarrow)}. \tag{3.8}$$

The reference quantity is the Coulombic Sherman function $S_{\rm coul}$, calculated from (3.2) and displayed in figure 4 at a collision energy of 5 MeV for both targets. A logarithmic scale is used (and hence $-S_{\rm coul}$ is shown) to demonstrate the strong increase of the spin asymmetry with scattering angle. It should be noted that $|S_{\rm coul}|$ is much larger for ^{208}Pb, since the spin asymmetry increases with nuclear charge due to the stronger relativistic effects in the electron-nucleus encounter. The steep decrease of $|S_{\rm coul}|$ for ^{208}Pb at forward angles is due to a zero at 31.5°, caused by the diffraction effects.

Calculating S from (3.3) and noting that $W_{fi}^{\rm soft}$ is spin-independent, the factor $(1 + W_{fi}^{\rm soft})$ in ${\rm d}\sigma^C/{\rm d}\Omega_f$ drops out (if $\tilde{A}_{fi}^{\rm vs(2)}$ is omitted), such that S becomes independent of bremsstrahlung, hence independent of the cut-off frequency ω_0 and therefore independent of the detector resolution. This was already stated by Johnson *et al* [33] who calculated the QED corrections to S within the second-order Born approximation in the Coulomb field. Numerical investigations indicate that the independence of bremsstrahlung holds even despite the consideration of the magnetic vs contribution. It should also be noted that S, when obtained from the distortion-modified Born cross section, is approximately equal to $S_{\rm coul}$, since ${\rm d}\sigma^{B1-C}/{\rm d}\Omega_f \sim {\rm d}\sigma^{\rm coul}/{\rm d}\Omega_f$, and the only additional dependence on the electron spin polarization is due to R_{fi}.

The modification of the spin asymmetry by the QED corrections, relative to $S_{\rm coul}$, is calculated from

$${\rm d}S = \frac{S}{S_{\rm coul}} - 1. \tag{3.9}$$

This means that in the Born approximation, the QED changes of $S_{\rm coul}$ are close to zero. In this context our previous Born results for ${\rm d}S_{\rm vsb}$ [13] should only be considered as qualitative

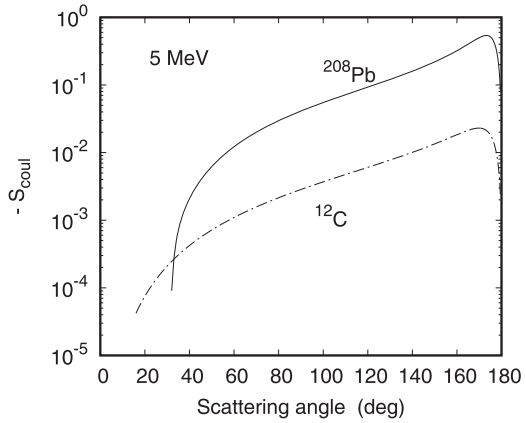

Figure 4. Coulombic Sherman function $-S_{\rm coul}$ for 5 MeV electrons colliding with ^{12}C ($-\cdot-\cdot-$) and ^{208}Pb (————) as a function of scattering angle ϑ_f.

estimates, since Coulomb distortion was not included in the contributions from vs and from soft bremsstrahlung.

When the phase-shift analysis is applied to the calculation of the cross section (which is the case when $A_{fi}^{\rm vs(2)}$ is omitted), S can be expressed in terms of the direct (A) and spin-flip (B) parts of the respective scattering amplitude [16, 18],

$$S = \frac{2{\rm Re}\{AB^*\}}{|A|^2 + |B|^2}. \tag{3.10}$$

Figure 5 depicts the change dS for ^{12}C and for ^{208}Pb at 5 MeV by means of the QED effects. Like in the case of the cross section modifications, the effect of vacuum polarization is small, at most 1%. The vs contribution is again of opposite sign and considerably larger in magnitude. The influence of the magnetic vs contribution on the spin-asymmetry change is negligibly small (<0.1% for $\vartheta_f \lesssim 140°$, up to 0.5% at $\vartheta_f \sim 170°$). The strong increase of $|{\rm d}S|$ for ^{208}Pb below 40° is caused by the zero in $S_{\rm coul}$ where the definition (3.9) is no longer meaningful.

The energy dependence of dS at the angle corresponding to the extremum of $S_{\rm coul}$ at 5 MeV impact energy (170° for ^{12}C, 173° for ^{208}Pb) is displayed in figure 6. For ^{208}Pb, $|{\rm d}S_{\rm vac+vs}|$, resulting from vacuum polarization and the vs correction, increases with $E_{\rm i,kin} = E_i - c^2$ up to 30° and then decreases, eventually oscillating with energy due to the onset of diffraction. In contrast, for the ^{12}C nucleus where diffraction starts only well above 100 MeV, there is a monotonous increase of $|{\rm d}S_{\rm vac+vs}|$ with energy. Due to numerical instabilities for the low-Z ^{12}C nucleus in the backward hemisphere (leading to wiggles), an energy above 40 MeV was not considered.

3.3. Dispersion effects

Dispersion effects result from the transient excitation of the target nucleus during the collision. For obtaining the transition amplitude $A_{fi}^{\rm box}$ for dispersion, calculated in the second-order Born approximation according to the Feynman box diagram [19], the sum over the excited nuclear states is in early work [34–36] evaluated with the help of a closure approximation.

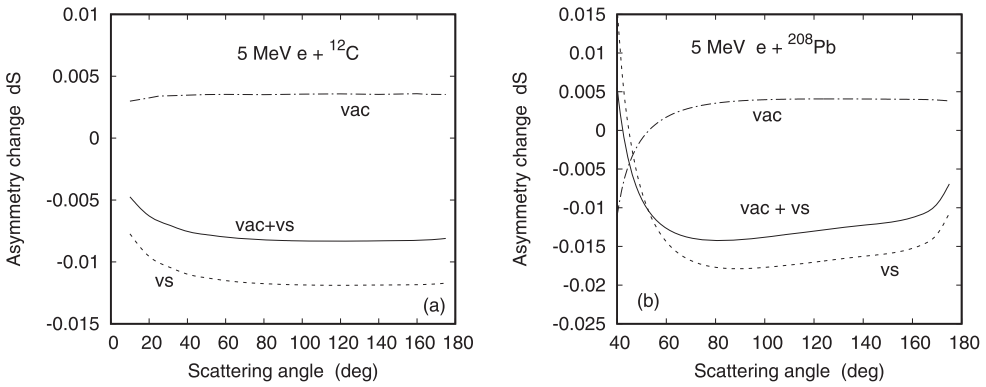

Figure 5. Relative change dS of the Sherman function in 5 MeV (a) e+^{12}C and (b) e+^{208}Pb collisions by the nonperturbative QED effects (d$S_{\rm vac+vs}$, ————) as a function of scattering angle ϑ_f. Also shown are the separate contributions from vacuum polarization (d$S_{\rm vac}$, $-\cdot-\cdot-$) and from the vs correction (d$S_{\rm vs}$, $-\,-\,-\,-$).

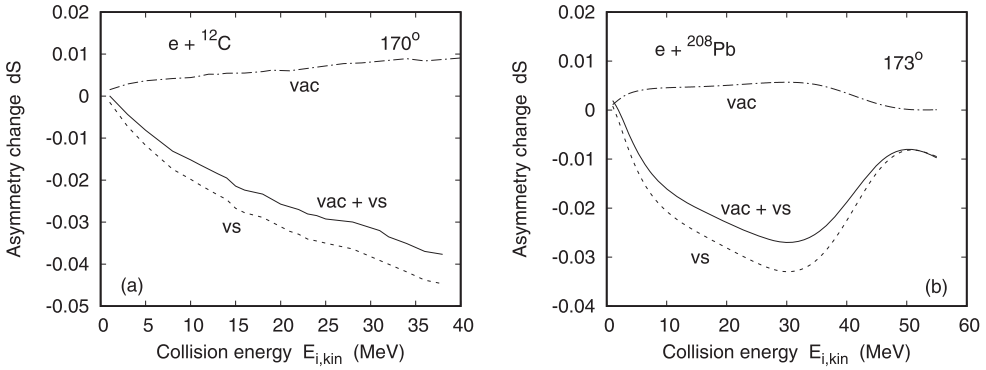

Figure 6. Relative change dS of the Sherman function (a) in e+^{12}C collisions at $\vartheta_f = 170°$ and (b) in e+^{208}Pb collisions at 173° by the nonperturbative QED effects (d$S_{\rm vac+vs}$, ————) as a function of collision energy $E_{\rm i,kin}$. Also shown are the separate contributions from vacuum polarization ($-\cdot-\cdot-$) and from the vs correction ($-\,-\,-\,-$).

A more refined approach takes the dominant excited states explicitly into account [37]. The required transition densities are obtained from the Hartree–Fock random phase approximation (HF-RPA [38]) and from the quasiparticle phonon model (QPM [39, 40]). In both prescriptions, the respective one-phonon states are calculated from the RPA equations pertaining to some nuclear model Hamiltonian. The QPM provides a refinement by accounting for the additional coupling to multi-phonon states. However, its effect on the excitation cross section is estimated to be small.

The cross section for elastic scattering, including dispersion to lowest order as well as the QED effects nonperturbatively, is given by

$$\frac{{\rm d}\sigma_{\rm tot}}{{\rm d}\Omega_f} = \frac{k_f}{k_i}\,\frac{1}{f_{\rm rec}}\sum_{\sigma_f}[\,|f_{\rm vac+vs}|^2(1\,+\,W_{fi}^{\rm soft})\,+\,2\,{\rm Re}\{f_{\rm coul}^{*}(\tilde{A}_{fi}^{\rm vs(2)}\,+\,A_{fi}^{\rm box})\}]. \tag{3.11}$$

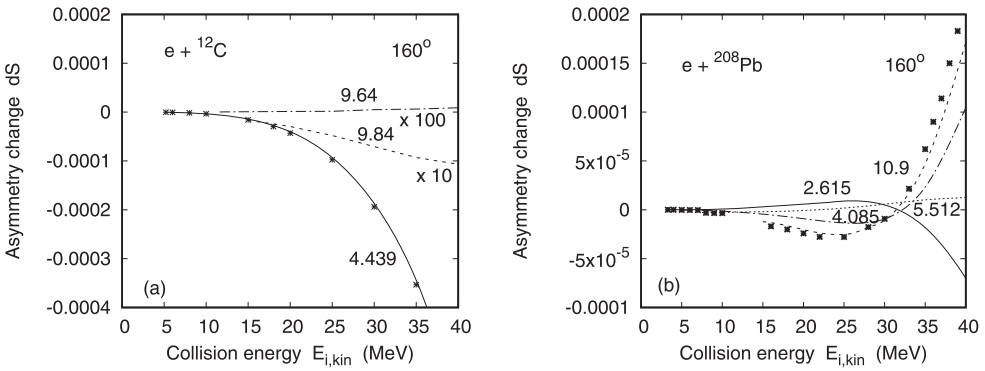

Figure 7. Relative change $\mathrm{d}S_{\mathrm{box}}(L,\,\omega_L)$ of the Sherman function (a) in $e+^{12}$C collisions and (b) in $e+^{208}$Pb collisions at $\vartheta_f = 160°$ as a function of collision energy $E_{\mathrm{i,kin}}$. In (a), the results for $\omega_L = 4.439$ MeV (————), 9.84 MeV (– – – –, multiplied by a factor of 10) and 9.64 MeV (– · – · –, multiplied by 100), and in (b), the results for $\omega_L = 2.615$ MeV (————), 4.085 MeV (– · – · –), 10.9 MeV (– – – –) and 5.512 MeV (⋯ ⋯) are shown. Included is their sum $\mathrm{d}S_{\mathrm{box}}$ (∗ ∗ ∗).

Without the QED effects, the cross section reduces to

$$\frac{\mathrm{d}\sigma_{\mathrm{box}}}{\mathrm{d}\Omega_f} = \frac{k_f}{k_i}\,\frac{1}{f_{\mathrm{rec}}}\sum_{\sigma_f}[\,|f_{\mathrm{coul}}|^2 \;+\; 2\,\mathrm{Re}\{f^*_{\mathrm{coul}}\,A^{\mathrm{box}}_{fi}\}], \tag{3.12}$$

leading via (3.9) with (3.8) to the dispersive spin-asymmetry change $\mathrm{d}S_{\mathrm{box}}$.

For ^{12}C, two dominant giant-dipole resonance states (at excitation energies $\omega_L = 23.5$ MeV and at 17.7 MeV) as well as two quadrupole states (at 4.439 MeV and 9.84 MeV) and two octupole states (at 9.64 MeV and 14.8 MeV) are considered in the sum over the nuclear excitations. The nuclear structure of the dipole states and of the 2^+_1 state is obtained from the QPM, and of the higher $L = 2$ and $L = 3$ states from the HF-RPA. The separate contributions of the three lowest states at 160° are shown in figure 7(a). At low impact energies the 4.439 MeV state gives by far the largest contribution to $\mathrm{d}S_{\mathrm{box}}$.

For ^{208}Pb, ten excited states with angular momentum $L \leqslant 3$ are included [41]. Except for the dipole states at 5.512 MeV and 14.2 MeV, they were calculated from the HF-RPA. The separate contributions of the four lowest states (at 5.512 MeV ($L = 1$); 4.085 MeV and 10.9 MeV ($L = 2$); and 2.615 MeV ($L = 3$)) are displayed in figure 7(b).

At impact energies up to 100 MeV the dispersive cross section modifications are small (at most 1%), such that the contributions from the individual excited states to the spin-asymmetry change are additive,

$$\mathrm{d}S_{\mathrm{box}} \;\approx\; \sum_{L,\omega_L} \mathrm{d}S_{\mathrm{box}}(L,\,\omega_L). \tag{3.13}$$

For such small cross section changes the spin-asymmetry modifications from the QED processes and from dispersion are also additive,

$$\mathrm{d}S_{\mathrm{tot}} \;\approx \mathrm{d}S_{\mathrm{vac+vs}} \;+\; \mathrm{d}S_{\mathrm{box}}\,\frac{1}{1+\Delta\sigma^C}, \tag{3.14}$$

where $\Delta\sigma^C$ is the cross section change by the QED effects (3.7), and $\mathrm{d}S_{\mathrm{vac+vs}}$ is the QED-induced change of the Sherman function.

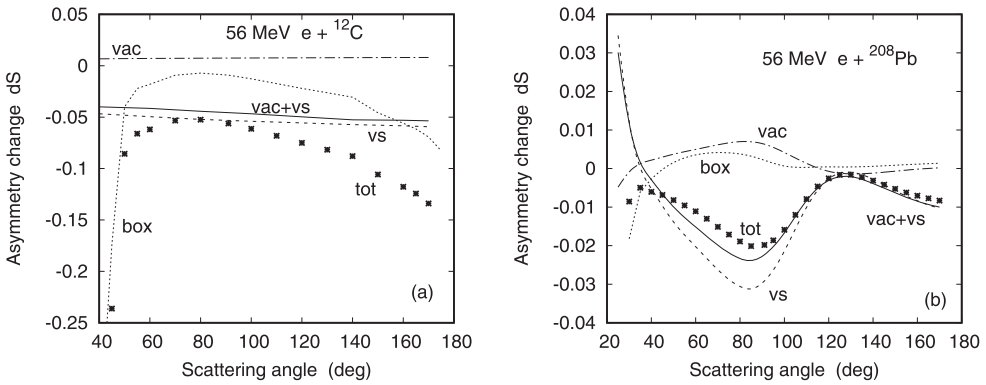

Figure 8. Relative change $\mathrm{d}S_{\rm tot}$ of the Sherman function in 56 MeV (a) $e+^{12}$C and (b) $e+^{208}$Pb collisions by the nonperturbative QED effects and dispersion ($***$) as a function of scattering angle ϑ_f. Also shown are the separate contributions $\mathrm{d}S_{\rm vac}$ ($-\cdot-\cdot-$), $\mathrm{d}S_{\rm vs}$ ($----$), $\mathrm{d}S_{\rm vac+vs}$ (————) and $\mathrm{d}S_{\rm box}$ ($\cdots\cdots$).

For collision energies below 12 MeV, the dispersive contribution to dS is of the order of 10^{-5} and thus negligibly small. However, at high energies dispersion can have quite a large influence on the spin asymmetry. From figure 8, where the angular dependence of the ^{12}C and ^{208}Pb spin-asymmetry change at 56 MeV is shown, it follows that the deviation of $\mathrm{d}S_{\rm tot}$ from $\mathrm{d}S_{\rm vac+vs}$ can be formidable. This is particularly true for the ^{12}C nucleus where dispersion is largely dominating at the smaller angles.

3.4. Accuracy of the spin asymmetry for lead and gold at 5 MeV

For the ^{208}Pb nucleus, a collision energy of 5 MeV and an observation angle of 173° (the parameters for the planned spin-asymmery measurement at MESA), the leading-order result for the Sherman function is $S^{(0)}_{\rm coul} = -0.5391$ and the spin-asymmetry change by the QED effects (with $A^{\rm vs(2)}_{fi}$ omitted) amounts to $\mathrm{d}S^{(0)} = -8.20\times10^{-3}$, which results in $S^{(0)}_{\rm tot} = -0.5347$. For ^{197}Au (which is favoured by the experimentalists) under the same kinematical conditions one has $S^{(0)}_{\rm coul} = -0.5158$ and $\mathrm{d}S^{(0)} = -7.28\times10^{-3}$, such that $S^{(0)}_{\rm tot} = -0.5120$. Let δS_0 be the uncertainty of $S_{\rm coul}$ and δS_1 the one of $\mathrm{d}S$ for this experimental setting. Then one has

$$S_{\rm tot} = S_{\rm coul}\,(1+\mathrm{d}S) = S^{(0)}_{\rm coul}(1\pm\delta S_0)[1+\mathrm{d}S^{(0)}(1\pm\delta S_1)]$$

$$\approx S^{(0)}_{\rm coul}\,[1+\mathrm{d}S^{(0)}\pm\delta S_0\pm\mathrm{d}S^{(0)}(\delta S_0+\delta S_1)], \tag{3.15}$$

such that the total inaccuracy $\delta S_{\rm tot}$ is obtained from equating (3.15) with $S_{\rm tot} = S^{(0)}_{\rm tot}(1\pm\delta S_{\rm tot})$,

$$\delta S_{\rm tot} \approx \frac{S^{(0)}_{\rm coul}}{S^{(0)}_{\rm tot}}\,[\delta S_0+\mathrm{d}S^{(0)}(\delta S_0+\delta S_1)] \approx \delta S_0+\mathrm{d}S^{(0)}\,\delta S_1. \tag{3.16}$$

The following processes contribute to the uncertainty of $S_{\rm coul}$.

(i) Numerical accuracy of the phase-shift analysis. Due to the convergence acceleration, the uncertainty in the backward hemisphere (up to $\vartheta_f\sim179°$) is about 10^{-9}.

(ii) Recoil. In order to validate the methods for including recoil, the target mass was set to infinity, thereby excluding any recoil effects. The change in $S_{\rm coul}$ from proceeding to the no-recoil results is about 10^{-5}.

(iii) Magnetic scattering (only for ^{197}Au). Since its nuclear spin is $3/2$, there exists besides potential scattering also a contribution to elastic scattering from the current-current interaction between electron and target nucleus. Due to the low magnetic moment of the gold nucleus this contribution is, however, completely negligible [8]. Note that its effect is of the order of the fine structure constant $(1/c)$ as compared to Z/c for potential scattering. Even for the ^{207}Pb nucleus with magnetic moment a factor of 4 larger, the magnetic scattering as estimated by DWBA [42] affects $S_{\rm coul}$ by less than 10^{-6} at a collision energy of 5 MeV and $\vartheta_f = 173°$.

(iv) Influence of atomic electrons. This is investigated in detail in [44], and the modifications of $S_{\rm coul}$ are estimated to add up to at most 6×10^{-4} [8].

(v) Nuclear charge distribution. For lead, a 17-term Fourier-Bessel parametrization is used. The replacement with a 13-term parametrization[25] induces in the backward hemisphere a change of less than 10^{-4}. (When compared with the less accurate Fermi distribution with parameters $r = 6.458$ fm, $a = 0.5234$ fm [43], the results at 173° would be modified by about 6×10^{-4}).
For ^{179}Au only the Fermi distribution is available. When the parameters used in the present work ($r = 6.38$ fm, $a = 0.535$ fm [25]) are replaced by those from [44] ($r = 6.44$ fm, $a = 0.5819$ fm), the respective change is about 5×10^{-4}.

For the uncertainty of the spin-asymmetry change the following processes have to be considered.

(i) Dispersion. This effect contributes less than 5×10^{-5} [see figure 7(b)].

(ii) Numerical accuracy of the phase-shift analysis when the QED potentials are present. For ^{208}Pb, this is estimated to be around 4×10^{-4}, for ^{197}Au it is about 8×10^{-4} at 173°.

(iii) Polarization of the nucleus by the impinging electron. This effect will modify the nuclear charge distribution. We estimate its contribution to be of the same order as when changing the parametrization of the charge distribution at arbitrary angles (about 2×10^{-3}).

(iv) Magnetic contribution to $A_{fi}^{\rm vs}$. Its effect is small at energies above 20 MeV or angles below 150°. However, at 5 MeV and 173° it affects the spin-asymmetry change by the vs process by about 5×10^{-3}, irrespective of nuclear charge.

(v) Detector resolution. This affects theory by means of the cut-off frequency for the soft bremsstrahlung. The influence of bremsstrahlung results, however, exclusively from the presence of the magnetic term $A_{fi}^{\rm vs(2)}$ (since dispersion is basically absent). For detector resolutions $0.2\% \lesssim \Delta E/E \lesssim 1\%$ its contribution is around 5×10^{-4}.

An addition of these uncertainties leads for ^{208}Pb to $\delta S_0 \lesssim 7.1 \times 10^{-4}$ and $\delta S_1 \lesssim 7.9 \times 10^{-3}$, resulting in a total uncertainty $\delta S_{\rm tot} \lesssim 0.08\%$. For ^{197}Au, these numbers are $\delta S_0 \lesssim 1.11 \times 10^{-3}$, $\delta S_1 \lesssim 8.3 \times 10^{-3}$ and $\delta S_{\rm tot} \lesssim 0.12\%$. We note that the total uncertainty is to a large extent due to inaccuracies of the nuclear charge distribution. For ^{197}Au, a somewhat smaller scattering angle (around $130° - 160°$) would increase the number from 5×10^{-4} to 2×10^{-3}, resulting in $\delta S_{\rm tot} \lesssim 0.26\%$, while for ^{208}Pb there would be no change.

4. Conclusion

The QED corrections to the elastic electron scattering cross section and to the Sherman function were estimated by using a nonperturbative approach in terms of a suitable potential

for the main part of the vertex and self-energy correction, together with the Uehling potential for vacuum polarization. The representation of the complete vs correction by a suitable potential is hampered by the presence of the magnetic contribution. However, this contribution can safely be neglected for collision energies near and above 30 MeV, and even at an energy as low as 5 MeV, the modification of the cross section change is at most 10% for ^{208}Pb and 20% for ^{12}C.

When investigating electron scattering from the ^{12}C nucleus, the deviations of the nonperturbative results from the respective Born predictions for the relative cross section change are mostly not exceeding 5%, such that the Born approximation is basically justified for a light nucleus like carbon. In case of the lead target, the differences to the Born QED results are quite large, enhancing the cross section change on the average by 60%.

One has to keep in mind that the size of the total QED corrections to the cross section depends strongly on the contribution of the soft bremsstrahlung, which in turn is controlled by the resolution of the electron detector.

The nonperturbative consideration of the vacuum polarization and the vs effect allows also for a consistent estimate of the QED-modified Sherman function. If the QED corrections were calculated from the Born approximation, they would not lead to any change in the spin asymmetry. In fact, the magnetic vs term is irrelevant for the spin-asymmetry change, its omission affecting the results in general by less than 0.1%, increasing to about 0.5% at the lowest energies and largest angles considered. For low collision energies, the spin-asymmetry changes dS by the QED effects increase strongly with energy (as long as diffraction plays no role). For lead this holds up to about 30 MeV at backward angles which are of particular interest to the experimentalists due to the large values of the spin asymmetry. The numerical accuracy of dS for carbon is unfortunately quite poor, partly due to the small absolute values of S (in the forward regime), and partly due to numerical instabilities when solving the Dirac equation (in the backward hemisphere). It amounts up to 0.5% at 3 MeV and 3% at 10 MeV, deteriorating to about 15% at 56 MeV. For lead, the results are stable, with an accuracy of $\lesssim$0.25% at 30 MeV and $\lesssim$1% at 56 MeV. For the determination of the degree of beam polarization at 5 MeV from experiment, the use of the calculated Sherman function at maximum spin asymmetry (173° for a gold or lead target) is subject to a total theoretical uncertainty below 0.15%.

We have also investigated the ratio between the modifications by the vertex and self-energy correction and those by vacuum polarization. The two processes lead in most cases to corrections of opposite sign. The vs process is often largely dominating the changes of the cross section and of the spin asymmetry. However, their ratio is strongly dependent on collision energy and scattering angle. It ranges mostly between 2 and 7, in contrast to earlier predictions that it is around 2.5.

Dispersion effects were taken into account by explicitly considering the dominant nuclear excitations with multipolarity 1,2 and 3. For collision energies up to 56 MeV, the cross section changes are at most 5×10^{-4} and 3×10^{-3} for ^{12}C and ^{208}Pb, respectively. The spin-asymmetry changes are tiny up to 10 MeV but increase strongly when the high-lying dipole states come into play, being particularly large for ^{12}C and small scattering angles.

Acknowledgments

I would like to thank C Sinclair, K Aulenbacher and P A Amundsen for fruitful discussions. I am also indepted to X Roca-Maza and V Yu Ponomarev for providing the nuclear transition densities required for dispersion.

Data availability statement

All data that support the findings of this study are included within the article (and any supplementary files).

ORCID iDs

D H Jakubassa-Amundsen https://orcid.org/0000-0002-9782-3796

References

[1] Abrahamyan S *et al* 2012 *Phys. Rev. Lett.* **108** 112502
[2] Chen J *et al* 2014 arXiv:1409.7741 [nucl-ex]
[3] Benesch J *et al* 2014 arXiv:1411.4088 [nucl-ex]
[4] Aulenbacher K, Chudakov E, Gaskell D, Grames J and Paschke K D 2018 *Int. J. Mod. Phys.*E **27** 1830004
[5] Adhikari D *et al* 2022 *Phys. Rev. Lett.* **128** 142501
[6] Aulenbacher K 2011 *Hyperfine Interact.* **200** 3
[7] Dehn M *et al* 2022 *Proc. of the 13th Int. Particle Acc. Conf. (IPAC2022) (Bangkok, Thailand)* 307
[8] Grames J M *et al* 2020 *Phys. Rev.*C **102** 015501
[9] Thapa R, Aulenbacher K and Tioukine V 2022 *Proc. of the 19th workshop on Polarized Sources, Targets and Polarimetry, PoS (PSTP2022)* 027
[10] Uehling E A 1935 *Phys. Rev.* **48** 55
[11] Soff G and Mohr P J 1988 *Phys. Rev.*A **38** 5066
[12] Shabaev V M, Yerokhin V A, Beier T and Eichler J 2000 *Phys. Rev.*A **61** 052112
[13] Jakubassa-Amundsen D H 2021 *Eur. Phys. J.*A **57** 22
[14] Tsai Y-S 1960 *Phys. Rev.* **120** 269
[15] Maximon L C and Tjon J A 2000 *Phys. Rev.*C **62** 054320
[16] Motz J W, Olsen H and Koch H W 1964 *Rev. Mod. Phys.* **36** 881
[17] Koshchii O, Gorchtein M, Roca-Maza X and Spiesberger H 2021 *Phys. Rev.*C **103** 064316
[18] Berestetskii V B, Lifshitz E M and Pitaevskii L P 1982 *Quantum Electrodynamics (Course of Theoretical Physics)* vol 4 2nd edn (Elsevier) 37, 98, 114f
[19] Bjorken J D and Drell S D 1964 *Relativistic Quantum Mechanics* (McGraw-Hill)
[20] Bucoveanu R-D and Spiesberger H 2019 *Eur. Phys. J.*A **55** 57
[21] Vanderhaeghen M, Friedrich J M, Lhuillier D, Marchand D, Van Hoorebeke L and Van de Wiele J 2000 *Phys. Rev.*C **62** 025501
[22] Tsai Y-S 1961 *Phys. Rev.* **122** 1898
[23] Yennie D R, Frautschi S C and Suura H 1961 *Ann. Phys. (NY)* **13** 379
[24] Klarsfeld S 1977 *Phys. Lett.* **66B** 86
[25] De Vries H, De Jager C W and De Vries C 1987 *At. Data Nucl. Data Tables* **36** 495
[26] Salvat F, Fernández-Varea J M and Williamson W Jr. 1995 *Comput. Phys. Commun.* **90** 151
[27] Yennie D R, Ravenhall D G and Wilson R N 1954 *Phys. Rev.* **95** 500
[28] Meister N T and Griffy T A 1964 *Phys. Rev.* **133** B1032
[29] Maximon L C 1969 *Rev. Mod. Phys.* **41** 193
[30] Weinberg S 1965 *Phys. Rev.* **140** B516
[31] Low F E 1958 *Phys. Rev.* **110** 974
[32] Yerokhin V A and Shabaev V M 1999 *Phys. Rev.*A **60** 800
[33] Johnson W R, Carroll C O and Mullin C J 1962 *Phys. Rev.* **126** 352
[34] Schiff L I 1955 *Phys. Rev.* **98** 756
[35] Lewis R R 1956 *Phys. Rev.* **102** 544
[36] Friar J L and Rosen M 1974 *Ann. Phys.* **87** 289
[37] Jakubassa-Amundsen D H 2022 *Phys. Rev.*C **105** 054303
[38] Roca-Maza X, Brenna M, Agrawal B K, Bortignon P F, Colò G, Cao Li-Gang, Paar N and Vretanar D 2013 *Phys. Rev.*C **87** 034301
[39] Ryezayeva N *et al* 2002 *Phys. Rev. Lett.* **89** 272502

[40] Ponomarev V Yu, Jakubassa-Amundsen D H, Richter A and Wambach G 2019 *Eur. Phys. J.*A **55** 236
[41] Jakubassa-Amundsen D H and Roca-Maza X 2023 *Phys. Rev.*C **108** 034314
[42] Jakubassa-Amundsen D H 2014 *J. Phys.*G **41** 075103
[43] Uginčius P, Überall H and Rawitscher G H 1970 *Nucl. Phys.*A **158** 418
[44] Roca-Maza X 2017 *Europhys. Lett.* **120** 33002